Int J Earth Sci (Geol Rundsch) (2004) 93:475–486
DOI 10.1007/s00531-004-0403-x

ORIGINAL PAPER

I. Görz · K. Bombach · U. Kroner · K. S. Ivanov

Protolith and deformation age of the Gneiss-Plate of Kartali in the southern East Uralian Zone

Received: 20 May 2003 / Accepted: 7 June 2004 / Published online: 27 August 2004

Abstract The southern East Uralian Zone consists of granite-gneiss complexes that are embedded in geological units with typical oceanic characteristics. These gneisses have been interpreted as parts of a microcontinent that collided during the Uralian orogeny. The gneiss-plate of Kartali forms the south eastern part of the gneiss mantle surrounding the Dzhabyk pluton. Its post-collisional protolith age of 327±4 Ma is inconsistent with the microcontinent model. The deformation of the gneisses took place in 290±4 Ma at the time of the intrusion of the Dzhabyk magmas. Granites and gneisses cooled and were exhumed together. Therefore, we interpret the gneiss complexes of the East Uralian Zone as marginal parts of the granitic batholiths that were deformed during the ascent and emplacement of the pluton. From Nd and Sr isotope constraints we conclude that the magma source of the gneiss protolith was an island arc. Since no evidence for old continental crust has been discovered in the East Uralian Zone, the Uralian orogeny can no longer be interpreted as a continent-island arc-microcontinent collision. Instead, the geochemical data presented within this paper indicate that the stacking and thrusting of island arc complexes played an important role in the Uralian orogeny.

Keywords Southern Urals · Gneisses · Geochronology · Temperature/time-path · Microcontinent

I. Görz (✉) · K. Bombach · U. Kroner
Institut für Geologie und Mineralogie,
TU Bergakademie Freiberg,
Cottastr. 2, 09596 Freiberg, Germany
e-mail: goerz@geo.tu-freiberg.de
Tel.: +49-3731-393160
Fax: +49-3731-393597

K. S. Ivanov
Institute for Geochemistry and Geology,
Russian Academy of Sciences,
Pochtovy Per. 7, 620151 Ekaterinburg, Russia

Introduction

The Urals are part of the Altaid tectonic collage surrounding the southern and western margins of the Angara-craton. The Altaids are mainly composed of material commonly found in subduction-accretion complexes. Gneiss-terranes, which are typical parts of most orogens, are almost totally missing (Sengör et al. 1993).

Also, the Westsibirian Lowlands which cover the area between the Urals and the Yenisey are composed of geological units that form in oceanic and island arc settings: volcanic arcs, accretion complexes, marine sediments and ophiolite sequences. However, at their western margin several gneiss terranes can be found in the East Uralian Zone forming exotic crustal units. They represent blocks of continental crust that are embedded in the oceanic units. The gneiss complexes are lined up in the hinterlands of the Magnitogorsk island arc. They are associated with Upper Carboniferous to Permian granites, thus composing granite-gneiss complexes and forming the Uralian Granite Axis. These blocks of continental crust cover approximately 30% of the East Uralian Zone. They reveal an assemblage of oceanic and continental crust that is unique in the whole Westsibirian Lowlands.

Since large gneiss-terranes usually represent fragments of former continental crust incorporated in the orogenic belts and metamorphosed under high P and T conditions, the East Uralian gneisses have been interpreted as a microcontinental block that collided the Magnitogorsk island arc during the Uralian orogeny and were affected by an intensive palingenesis which resulted in the formation of the late Palaeozoic batholiths. According to this model, the gneisses are the country rock of the granites (Berzin et al. 2001).

However, this model is inconsistent with geochemical and geophysical data. Nd-isotope data from Gerdes et al. (2002) document a crustal residence time that is too brief to support the microcontinental concept. The crustal density below the East Uralian Zone is significantly higher than in a typical continental crust (Döring & Götze 1999).

While age data from the Middle Urals provides evidence that the gneisses have formed during the Uralian orogeny in the Southern Urals the confirmation whether or not they present a pre-Cambrian microcontinent has not yet been addressed. Nevertheless, the gneisses occupy a key position for the reconstruction of the tectonic history of the Urals. Therefore, age determination in these rocks can provide essential constraints for a geodynamic model that includes geochemical and geophysical data and is consistent with the Altaid model of Sengör et al. (1993).

Background

Geological Setting

All East Uralian granite-gneiss complexes have a similar architecture. They consist of HT/LP metamorphic gneisses that surround granite plutons and are associated with N-S striking shear zones.

The largest gneiss area of the southern East Uralian Zone is the gneiss-plate of Kartali, east of the city of Magnitogorsk (Fig. 1). It has a NE-SW extension of 20 km, a SE-NW extension of 10 km and is part of the gneisses surrounding the Dzhabyk granite, the largest batholith of the southern East Uralian Zone. The gneiss-plate of Kartali forms the roof of the Dzhabyk pluton and is composed of deformed granites that contain mafic and metapelitic inclusions. The Dzhabyk granite, which is a two mica granite, is situated in the NE of the gneiss-plate. It has a crystallization age of 291±4 Ma (Montero et al. 2000). The granites of the Dzhabyk pluton continuously transform to the gneisses of Kartali. Sharp contacts and contact metamorphic mineral associations cannot be found. The strain intensity increases to the SE. Granites of a platy disposition and discrete shear zones, augengneisses with an anastomosing foliation and ultramylonites with a parallel foliation form a series of rocks with an increasing grade of deformation. Two granite lenses are included in the gneiss-plate, both of them are also continuously transforming to gneisses.

The gneiss-plate of Kartali is characterized by a foliation that strikes concordantly to the margin of the Dzhabyk pluton and dips to the S or E at angles of less than 30°. These structures have a non-conform orientation to the regional framework of the East Uralian Zone that strikes N-S and dips steeply.

In the E the gneiss-plate of Kartali adjoins the oceanic units of the East Uralian Zone. These oceanic units comprise of mafic and ultramafic metamorphic rocks representing oceanic lithosphere and marine fine-clastic sediments of Cambrian to Lower Carboniferous age. The sediments were metamorphosed in strike-slip belts and in the vicinity of the granite-gneiss complexes, but remained non-metamorphic outside of these zones (Kisters et al. 1999). The contact of the gneiss-plate with the oceanic units is sharp. Serpentinites and amphibolites that are exposed in the NE contain synkinematic veins with granitic filling that verifies the intrusive relationship of both rocks. Fine-grained graywackes, so-called 'aleurolithes' of Lower Carboniferous age are exposed in the SE. They were progradely metamorphosed at the contact. The metamorphic growth of sillimanite, andalusite and biotite verifies the hot emplacement of the gneiss complex in these late Palaeozoic sediments.

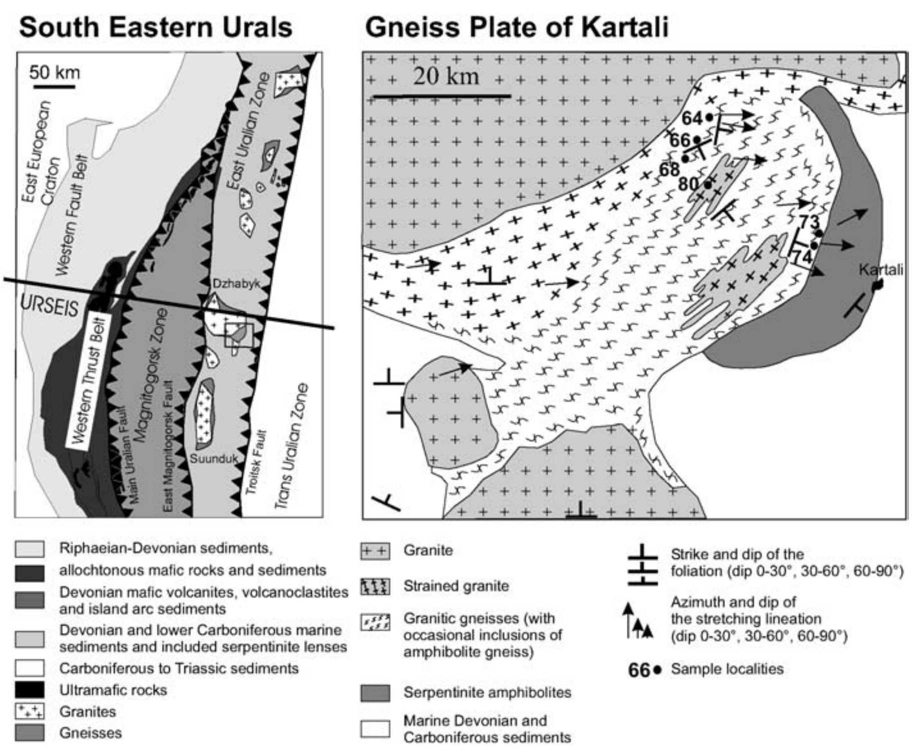

Fig. 1 Sketch map of the southern Urals and the gneiss-plate of Kartali

The fabric transformation is well documented in thin sections. Microcline is replaced by quartz and plagioclase, the granitic fabric resolves completely and a fine-grained parallel foliated fabric grows by recrystallization. The rocks underwent a simple retrograde path of metamorphism. The P/T–conditions were estimated by the comparison of appearing mineral phases with experimentally calibrated phase diagrams after Spear (1993) at a temperature range of 550–600°C and a pressure of 2–3 kbar.

The results of our literature enquiries, field research and microstructural analysis are inconsistent with the microcontinental model. Therefore, the following scenario is suggested to explain the formation of the gneiss-plate of Kartali: The gneisses represent deformed marginal sections of the Dzhabyk granite and their formation was associated with the ascent of the pluton. If this is true, then the gneisses should be of Carboniferous or Permian age. In fact, there is not a single age date published supporting the microcontinental model.

Our geochronological investigation aims to determine the crystallization age of the gneiss protolithes and of the deformation, to reconstruct the exhumation history of the gneiss-plate and to discover evidence for the magma source of the granite-gneiss complexes.

Sampling

In order to discover age differences depending on the grade of metamorphism of the gneisses the whole deformation series from an undeformed granite to a totally recrystallised ultramylonite has been sampled. All specimens have a granitic composition; therefore they contain only a limited spectrum of minerals. Quartz, plagioclase and microcline are the major constituents. Apatite, zircon, monazite and magnetite are accessory constituents. Mineral phases were selected for the purposes of dating, considering their behaviour during metamorphism and deformation, their isotope systems and the closure temperatures of the isotope systems. Zircons were used to determine the crystallization-ages, because all rocks contain prismatic magmatic zircons which crystallised below the closure temperature of its U/Pb- system. Only muscovite could be used to date the deformation of the gneisses, because it recrystallised totally during the deformation and its closure temperature of 550°C (Jäger 1973) is at the lower limit of the estimated deformation temperature. Biotite and K-feldspar with closure temperatures of 300 and 200°C respectively (Poty & Roth 1989) were used for dating cooling ages without a special geological significance.

Analytical methods

Four samples were studied by the Pb/Pb evaporation method, eight samples by the Rb/Sr method. Rock and mineral separation was carried out at the Westfälische Wilhems-Universität in Münster (Germany). Biotite and muscovite of size fractions 350–250 μm and 250–180 μm were separated from small parts (approximately 1 kg) of 8–12 kg samples collected for zircon separation. Each sample was crushed in a steel mortar and was further reduced in size by grinding for a few seconds in a tungsten carbide mill. Samples were sieved and fines were removed. Mica was enriched by standard methods, such as adherence to a piece of paper, Frantz magnetic separator and hand-picking under the binocular microscope. Possible contaminants were removed by grinding under ethanol in an agate mortar and pestle. The mica concentrates were washed in p.a. ethanol and three times distilled water in an ultrasonic bath.

Large K-feldspar crystals were carefully crushed by hammer, grinded in an agate mortar and cleaned of inclusions with a Frantz magnetic separator.

Zircons were enriched from the <350 μm size fraction by standard methods utilising a jaw-crusher, a roller-mill, a Wilfley table, magnetic and heavy liquid techniques. Then, they were sieved to size fractions of 180–350 and 150–180 μm and hand-picked. The zircons were studied under REM regarding their surface and internal structures at the TU Bergakademie Freiberg (Germany) to prove whether they were suitable for Pb/Pb analysis. Only prismatic zircons without cracks and inclusions were used for dating.

Whole rock powders were spiked with ^{87}Rb-^{84}Sr and ^{147}Nd spikes, mineral separates with ^{87}Rb-^{84}Sr spike. The mixtures were dissolved in screw-top Teflon vials using a 5:1 HF-HNO_3 mixture as dissolvent on a hot plate. Rb,Sr, Sm, Nd were separated in quartz glass columns using standard ion exchanging procedures.

Rb/Sr and Sm/Nd-analyses were carried out at the Westfälische Wilhelms-Universität Münster using a VG Sector 54 multi-collector mass-spectrometer for Sm, Nd and Sr and a NBS-type Teledyne mass-spectrometer for Rb. Based on the repeated analysed Rb-standard NBS 607 a mass discrimination factor of 0.9947 was used. Based on repeated measurements of the standard, the ^{87}Rb/^{86}Sr ratios were assigned with a 2σ uncertainty of 1%. Exponential mass fractionation correction was applied to Sr, Sm and Nd. For these isotope ratios, uncertainties are reported at the 2σ level taking into account the within-run error: An estimated uncertainty of 0.1% for the ^{87}Sr/^{86}Sr spike ratio; the error magnification based on spike/sample ratio and the blank correction. Isochrons were calculated using ISOPLOT/Ex2.06 (Ludwig 1999).

Lead evaporation of single zircons was carried out in the Isotope Lab of the Department for mineralogy at the TU Bergakademie Freiberg using a FINIGAN MAT 262 based on the studies of Kober (1986, 1987). Individual zircons were embedded into a rhenium filament for evaporation and heated up to 1,450°C in order to release lead from the metamict zones and impurities. After this cleaning process the zircon was heated up to 1,600°C. Thereby lead isotopes were evaporated in a single step and collected on a second rhenium filament. This lead was ionised at 1,180–1,260°C. Data record took place by magnetic peak switching of the mass sequence ^{206}Pb,

^{207}Pb, ^{204}Pb using an ion counter. The $^{207}Pb/^{206}Pb$ ages were calculated from the determined $^{207}Pb/^{206}Pb$ and $^{204}Pb/^{206}Pb$ ratios with the following corrections: (1) Common lead correction after Stacey and Kramers (1975) and (2) A specific mass spectrometer calibration factor (mass bias). The mass bias (0.36±0.22% amu) was calculated from the measurement of two standard zircons and includes the thermal fractionation of Pb and the mass bias of the ion counter.

Nd depleted mantle model ages were calculated after DePaolo & Wasserburg (1986) using $^{143}Nd/^{144}Nd_{mantle}$= 0.51316 and $^{147}Sm/^{144}Nd_{mantle}$=0.214.

Results

Zircon morphology

The size relations of zircon crystal faces are strongly dependent upon the chemistry of the growth medium (Benisek & Finger 1993) and on the temperature of the crystallizing medium (Pupin 1980).

In both granitic and gneissic samples zircons with almost equally developed [100]+[110] or [100]<[110] prism faces, dominant [101] pyramids and small or no [211] pyramid faces can be found. The zircon typology and the mean-points of the distribution after Pupin (1980) are equal for granites and gneisses, indicating that both rocks had a similar magma chemistry and crystallization temperature. The subtypes that were observed and the mean-points of the populations are to be found in Fig. 2.

In general two subpopulations can be distinguished. Subpopulation A comprises of euhedral, middle-prismatic zircons with a light-yellow and clear appearance. Most of the zircons have a length/width-ratio of 2 to 4. They have an oscillatory magmatic zoning, and 20% of the zircons contain cores. The cores are fragments of inherited zircons with sharp edges and a magmatic zoning which is clearly visible. The gneiss zircons were affected by the deformation in a destructive manner. Metamorphic crystal growth seldom occurs; evidence for recrystallization is missing totally. Fractures are the dominant structures within the mylonitic samples. More than 90% of the fractures incline discordantly to the crystal faces. While cracks are absent in the zircons from the granite, the number of fractures increases with the intensity of the strain. The fractures provide good conditions for fluid corrosion. The intact surface can be additionally corroded, and solution pits and raw surfaces form. These structures are more common the stronger a sample is deformed. Since Subpopulation A of the granites and gneisses is optically identical, but provides different ages, it has to be subdivided into an A1 subpopulation, including the zircons from the granite and an A2 subpopulation, including the zircons from the gneisses.

Subpopulation B is characterized by a dirty-yellow or brown colour and contains metamict areas without zoning. The zircons which are euhedral, have oscillatory zonations outside the metamict areas, and most of the zircons have a length/width-ratio of 2 to 4. Healed fractures and thin overgrowth can also be found.

Both populations are interpreted to be of igneous origin because of their euhedral shape and their oscillatory zoning. Most of the samples studied contain zircons of both groups. However, the granitic samples consist almost exclusively of group ‘A’ zircons, while in the gneisses group ‘B’ zircons occur more frequently.

To evaluate the geological significance of the measured ages, the disturbance of the isotopic system of a zircon must be taken into account. The group ‘A’ zircons

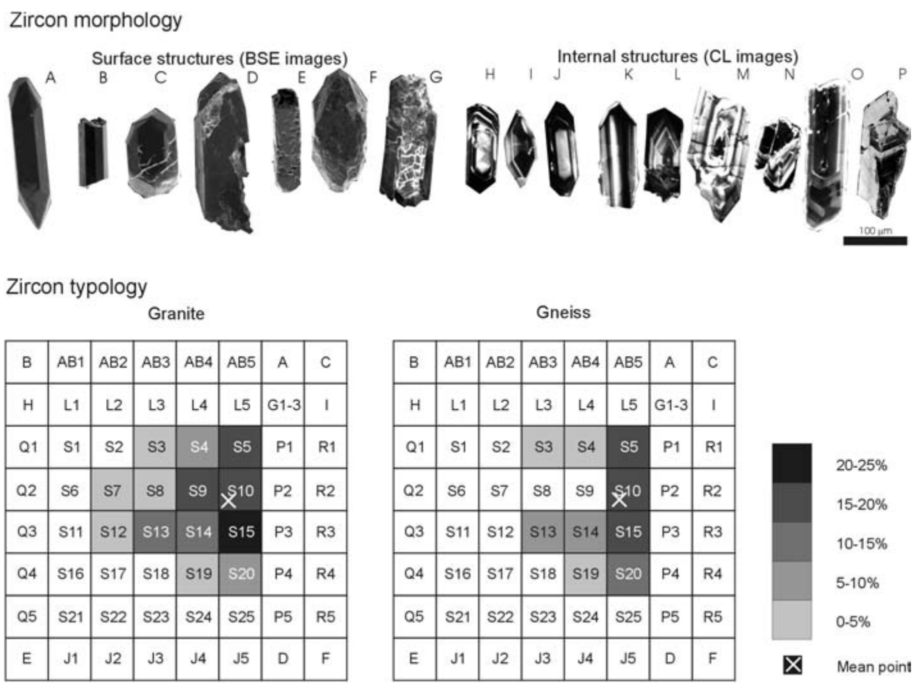

Fig. 2 Zircon morphology and typology after Pupin (1980), Internal structures of zircons (Cl images) of granites *H-I* and gneisses *K-P*. Photographs *K-P* show the influence of the deformation on gneiss zircons. Zircons *M-P* represent population B

Fig. 3 Single-zircon $^{207}Pb/^{206}Pb$ ages of the gneiss-plate of Kartali

do not contain metamict or recrystallised areas. Therefore, differences in the age information can be interpreted as the mixing of ages. In this case, the zircons contain an inherited core and provide an older age than the crystallization age of the magma. The group 'B' zircons contain metamict areas, as well as overgrowth. It is assumed that significant Pb-loss might have occurred and that the measured $^{207}Pb/^{206}Pb$ ages are only minimum values.

Pb/Pb geochronology

17 euhedral zircon grains without cracks and visible cores were analysed. They present a well centred and clearly separated age distribution (Fig. 3 and Table 1). The A1 granite zircons yield a mean age of 295±3 Ma and can be assigned to the second phase of Uralian plutonic activity Fershtater et al. (1997). The age is equal within error to that of the central Dzhabyk intrusive rocks dated at 291±4 Ma by Montero et al. (2000). Thus, the granites exposed in the gneiss-plate can be regarded as marginal parts of the Dzhabyk granite.

The A2 gneiss zircons yield a mean age of 327±4 Ma that corresponds with the age of the first phase of the Uralian plutonic activity Fershtater et al. (1997). This verifies that the gneiss protolith is not a part of a Precambrian continental basement, but a post-collisional intrusive rock.

The group B zircons have an average age of 451±6 Ma. These zircons are interpreted to be relics from the magma source of the gneiss protolith. Similar ages have been dated in syenites and gneisses in the Sisert and Salda complexes in the East Uralian Zone of the Middle Urals by Echtler et al. (1997), Kramm et al. (1993) and Frigberg et al. (2000).

Three zircons yield ages between 350–406 Ma and do not scatter around a mean. Probably, they give mixing ages between group 'A' and 'B'. One zircon has an age of 713±27 Ma. This age can not be assigned to a known geological event in the East Uralian Zone.

Rb/Sr geochronology

As has been mentioned in the above, the gneisses followed a simple retrograde path of metamorphism and were deformed at temperatures of 600–550°C. Therefore, in order to reconstruct the deformation and exhumation

Table 1 Pb isotope data of granites and gneisses from the gneiss-plate of Kartali

Kartali					
Sample	$^{204}Pb/^{206}Pb$	$^{207}Pb/^{206}Pb$	$^{207}Pb/^{206}Pb$ cor.	2σ	Age (Ma)
Group A1					
Mean age					295±>3
80a.1	0.00009	0.05341	0.05360	0.00015	299±7
80a.2	0.00011	0.05365	0.05384	0.00006	294±3
80a.3	0.00001	0.05232	0.05250	0.00081	299±35
66.2.1	0.00025	0.05580	0.05600	0.00022	298±8
73.3.1	0.00027	0.05594	0.05614	0.00037	292±18
Group A2					
Mean age					327±4
66.2.2	0.00016	0.05507	0.05527	0.00017	326±9
66.2.4	0.00012	0.05454	0.05474	0.00031	327±13
74.2.1	0.00026	0.05655	0.05676	0.00015	326±15
74.3.2	0.00017	0.05520	0.05540	0.00012	328±5
Group A3					
73.3.2	0.00024	0.06635	0.06313	0.00079	713±27
66.2.5	0.00011	0.05503	0.05362	0.00022	355±9
66.3.1	0.00025	0.05815	0.05477	0.00094	403±42
74.1.1	0.00020	0.05747	0.05484	0.00070	406±31
Group B					
Mean age					451±6
66.2.3	0.00101	0.07136	0.07161	0.00060	493±24
74.1.1	0.00021	0.05882	0.05903	0.00006	450±2
74.2.2	0.00017	0.05835	0.05856	0.00054	459±21
74.2.3	0.00024	0.05919	0.05941	0.00050	448±21
74.2.4	0.00004	0.05686	0.05707	0.00026	471±10
74.3.1	0.00021	0.05863	0.05884	0.00076	444±30

$^{207}Pb/^{206}Pb$ cor.: corrected for common lead after Stacey and Kramers (1975) and for mass bias

Table 2 Rb/Sr isotope data

Sample	Sr (ppm)	Rb (ppm)	$^{87}Rb/^{86}Sr$	$^{87}Sr/^{86}Sr$	2σ	Ini.$^{87}Sr/^{86}Sr$	Initial (Ma)
Kartali Granites							
58 Wr	183.4	196.1	3.1	0.71689	0.00002	0.70389	295
80a Wr	286.1	149.6	1.51	0.71099	0.00001	0.70463	295
80a Bi	3.1	1,018.9	1,437	6.09925	0.00043		
80a Kfs	417.5	212.6	1.47	0.71082	0.00005		
80b Wr	301.5	161.4	1.55	0.71129	0.00001	0.70479	295
80b Bi	5.5	945.6	603	2.98397	0.00005		
80b Kfs	417.5	212.6	0.901	0.70866	0.00005		
80c Wr	236.1	180.3	2.21	0.71329	0.00001	0.70401	295
80c Kfs	302.3	280.2	2.97	0.71588	0.00002		
Gneisses							
64 Wr	189.2	106.4	1.63	0.71385	0.00001	0.70627	327
64 Mus	15.2	384.2	88.7	1.06882	0.00002		
66 Wr	519.2	73.4	0.409	0.70747	0.00001	0.70557	327
66 Bi	6.9	768.3	368	2.10558	0.00005		
66 Mus	39.1	347.7	26.00	0.81174	0.00004		
66 Mus	40.4	346.6	25.1	0.80858	0.00003		
68 Wr	92.7	167.4	5.24	0.73017	0.00003	0.70580	327
68 Mus	7.8	621.1	202	1.54091	0.00002		
73 Wr	442.6	106.0	0.693	0.70870	0.00001	0.70547	327
73 Bi	16.6	705.9	129.2	1.20599	0.00046		
74 Wr	251.6	33.1	0.381	0.70730	0.00002	0.70553	327
74 Bi	8.7	580.7	209	1.50901	0.00009		
Suunduk Granites							
6/10 Wr	111.9	135.1	3.50	0.72016	0.00004	0.70573	290
10/4 Wr	170.3	259.6	1.90	0.71222	0.00003	0.70357	290
Gneisses							
8/8a Wr	137.5	35.9	0.76	0.70932	2.0798E-05	0.70620	290
10/5 Wr	57.5	163.3	8.26	0.74470	2.0551E-05	0.71064	290

Note: Bi — biotite; Kfs — K-feldspar; Mus — muscovite; Wr — whole rock; $^{87}Sr/^{86}Sr$ are normalized to $^{86}Sr/^{88}Sr$=0.1194

Table 3 Rb/Sr ages calculated with mineral-whole rock isochrons and mono-mineral isochrons

	Granite		Gneiss	
	Mono-mineral	Mineral-whole rock	Mono-mineral	Mineral-whole rock
Muscovite	–	–	290±3Ma MSWD=0.87 4 points	288±3Ma MSWD=244 7 points
Biotite	263±4Ma MSWD=0 2 points	265±3Ma MSWD=9.6 4 points	265±4Ma MSWD=0.25 3 points	269±3Ma MSWD=20 6 points
K-feldspar	–	237±5 Ma MSWD=0.68 4 points	–	238±17 Ma MSWD=135 7 points

MSWD — mean squared weighted deviates

history of the gneiss-plate we had to date cooling ages. The Rb/Sr method was used for dating whole rock powder, muscovite, biotite and K-feldspar (Table 2). Isochrons were separately calculated for granites and gneisses. Each mineral yields an age depending upon the closure temperature of its isotopic system. An overview is presented in Table 3 and Fig. 4.

Usually whole rock and mineral separate data are used to calculate an isochron. The determined whole rocks have a low $^{87}Rb/^{86}Sr$-ratio and fix the isochron near the origin. Furthermore, the whole rock $^{87}Sr/^{86}Sr$ ratios show, whether the samples were in equilibrium with each other. The regression of our samples was a line with a high MSWD that does not deserve the name isochron. Examining the data-points for the reason for the derivation, it was recognized, that the whole rocks follow a linear trend with a flatter slope than the micas. As a reason for this the low cooling rate of the gneiss-plate was considered. All samples contain at least 90% quartz and feldspars. The feldspars are relatively rich in Rb and have a very low closure temperature, which lies 100–150°C below biotite and 300–350°C below muscovite. Thus, the whole rock age corresponds to a low cooling temperature and is in good agreement with the K-feldspar age. The MSWD of a whole rock–mineral isochron is increasing with the difference in the closure temperatures of its components.

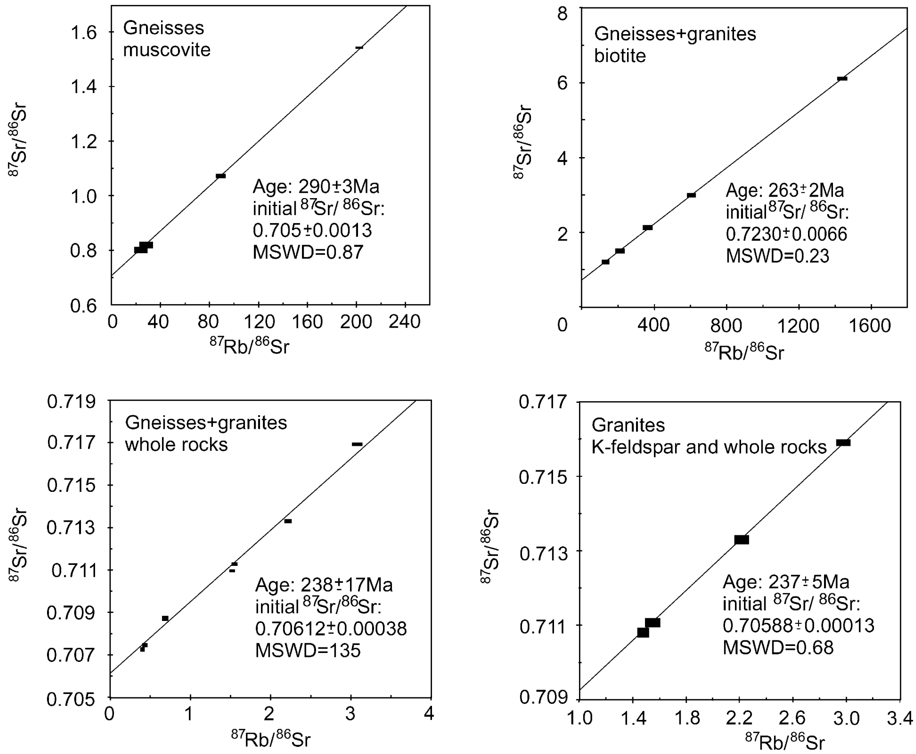

Fig. 4 Rb/Sr isochron diagrams for samples from the gneiss-plate of Kartali

Table 4 Initial $^{87}Sr/^{86}Sr$ ratios at the ages of mono-mineral isochrons

Age in Ma	Mean initial $^{87}Sr/^{86}Sr$	Maximum error of initials (%)	2 σ error of measurement (%)
290	0.70469	0.28	0.52
265	0.71859	0.18	0.58
263 (gneiss)	0.72371	0.33	0.71
263 (granite+gneiss)	0.72063	0.31	0.47
237	0.70579	0.002	0.58
238	0.70704	0.019	0.38

It is negligible for K-feldspar (MSWD=0.68), high for biotite (MSWD=20) and extremely high for muscovite (MSWD=244). Thus, it must be concluded, that only components of the same closure temperature are suitable to be calculated as an isochron. Therefore, K-feldspar is the only mineral that can be plotted with the whole rock. The mica isochrons were calculated without whole rocks.

The gneisses yield a muscovite age of 290±3 Ma and a biotite age of 265±3 Ma. The granites have a K-feldspar age of 237±5 Ma and a biotite age of 263±4 Ma. The biotite age of granites and gneisses is equal within error, so that both rocks can be plotted on a common isochron with 263±2 Ma. The whole rock isochron provides an age of 238±15 Ma.

The mono-mineral isochrons do not accurately determine the initial $^{87}Sr/^{86}Sr$ ratio of a system, because data-points near the origin are missing. Therefore, it has to be proven, whether rocks on the same isochron have similar initial $^{87}Sr/^{86}Sr$ ratios. Only in this case do they really have the same age. The initial $^{87}Sr/^{86}Sr$ ratio of each whole rock sample was calculated at the age of the respective isochron using the decay equation for Rb. If the initial $^{87}Sr/^{86}Sr$ ratios were statistically equal, they should scatter around a mean value. The best possible estimation of the initial $^{87}Sr/^{86}Sr$ ratio is dictated by the uncertainty of the measurements ($2\sigma_{87Rb/86Sr}$=1% and $2\sigma_{87Sr/86Sr}$=0.1%) and presented by the equation:

$$a = \left(2\sigma_{87Rb/86Sr} + 2\sigma_{87Sr/86Sr}\right)^{1/2}/n^{1/2}, \qquad (1)$$

where 'a' is the error, 'n' the number of data-points per isochron and σ the uncertainty of measurement. As seen in Table 4 all initial $^{87}Sr/^{86}Sr$ ratios lie in the interval given by the accuracy of the measurements. No additional statistical tests are necessary to prove the equality of the initial $^{87}Sr/^{86}Sr$ ratios.

The ages of mono-mineral isochrons and whole rock-mineral isochrons are almost the same (Table 3), but the MSWD of the mono-mineral isochrons are always <1, even if many data points have been plotted. Only the whole rock isochron has a very high MSWD=135, which may be caused either by an incomplete homogenisation of the magma, or by secondary alterations or by the differing contents of micas with high closure tempera-

Table 5 Sm/Nd isotope data of granites and gneisses from the gneiss-plate of Kartali and the gneiss-mantle of the Suunduk complex

Sample	Sm (ppm)	Nd (ppm)	$^{147}Sm/^{144}Nd$	$^{143}Nd/^{144}Sm$	(+/−2σ) 10E-6	Age t (Ma)	εNd (t)	T_{DM} (Ma)
Kartali								
58	4.86	33.77	0.0870	0.512513	25	295	1.77	766
80a	1.60	11.08	0.0871	0.512472	14	295	0.97	816
80b	4.14	29.90	0.0838	0.512493	2	295	1.50	771
73	2.80	18.70	0.0905	0.512365	8	327	-1.25	970
74	3.43	20.51	0.1010	0.512409	12	327	-0.80	1,001
Suunduk								
6/10	5.33	22.44	0.1436	0.512627	12	290	1.82	1,134
8/8a	3.20	12.98	0.1492	0.512670	15	290	2.45	1,131
10/5	2.20	10.66	0.1246	0.512597	7	290	1.96	945
10/4	2.90	15.75	0.1114	0.512541	4	290	1.38	906

Note: $^{143}Nd/^{144}Nd$ ratios were normalized to $^{146}Nd/^{144}Nd$=0.7219; $^{147}Sm/^{144}Nd$ ratios are assigned an uncertainity of 0.3%, the sample 80a an uncertainity of 0.7% at the 2σ level; Bulk Earth parameters used to calculate εNd are $(^{143}Nd/^{144}Nd)_{CHUR}$=0.51265, $(^{147}Sm/^{144}Nd)_{CHUR}$=0.1967

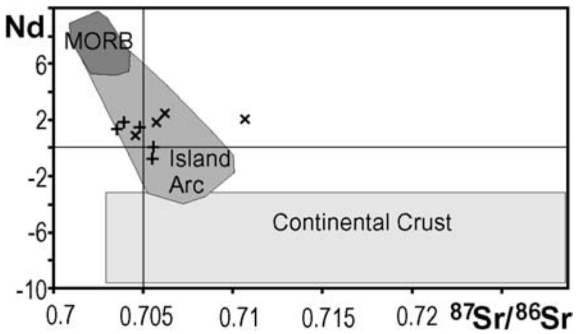

Fig. 5 Sr-Nd plot after White (1997) for initial isotope data from the gneiss-plate of Kartali *(+)* and from the gneiss mantle of the Suunduk complex *(x)*

tures, that slightly change the age information of the whole rock.

Sm/Nd isotope characteristics

Sm/Nd isotope data were determined by using whole rock samples only to calculate depleted mantle model ages. In addition to the samples from the gneiss-plate of Kartali five samples from the gneiss mantle of the Suunduk pluton south of the Dzhabyk were investigated (Table 5). All samples produced ages for the separation from the depleted mantle between 766–1,134 Ma. The mean age is 970 Ma. This short crustal residence time does not correspond with the formation of the gneisses from an old crustal block that broke off the East European Craton, whose consolidation was finished by 1.65 Ga (Giese et al. 1999). All rocks that were remelted from the East European Craton should have model ages higher than this.

The initial εNd values were calculated for the time of crystallization, for the Suunduk complex after Shenderowitsch (1965). They range from −2 to 2.5. In the Sr-Nd-isotope diagram after White (1997) nearly all samples lie in the island arc array, implicating that they have a juvenile source rock (Fig. 5). This data shows a good consensus with Gerdes et al. (2002), who published isotope data from the Dzhabyk pluton.

Discussion

Thermochronology

The granite enclaves in the gneiss-plate of Kartali have a crystallization age of 295±3 Ma. They represent marginal parts of the Dzhabyk granite (291±4 Ma after Montero et al. 2000), that are exposed in the gneiss-plate in a tectonic window.

The protolith of the gneisses crystallized in the Upper Carboniferous at 327±4 Ma. Owing to this young age it can be excluded that the gneisses are part of the Proterozoic cratonic basement or of any other microcontinent that collided during the Uralian collision.

The deformation age of the gneiss-plate of Kartali was determined by dating the recrystallised muscovites and comes to 290±3 Ma. This age corresponds to the crystallization age of the Dzhabyk pluton of 291±4 Ma. Therefore, it is assumed that the deformation of the gneiss-plate was correlated with the intrusion of the Dzhabyk batholith. However, what relation have both rocks and what has caused the gneissification of the oldest intrusive rocks of the Dzhabyk granite-gneiss complex?

In order to reconstruct the deformation and exhumation history of the gneiss-plate there has been drawn up a temperature-time path that correlates the tectonic evolution of a rock unit with its thermal history. The radiogenic ages of the samples were plotted against the closure temperatures of the isotope systems of the dated minerals. After Dodson (1973) the closure temperature is the temperature a sample had at the time of its apparent age. Experimentally determined closure temperatures depend on the grain size and the cooling rate and therefore differ slightly from author to author. Closure temperatures after Jäger (1973) and Poty & Roth (1989) were used as mentioned in the “Sampling” chapter .

Temperature-time paths have been worked out for several tectonic settings and can be used for their dis-

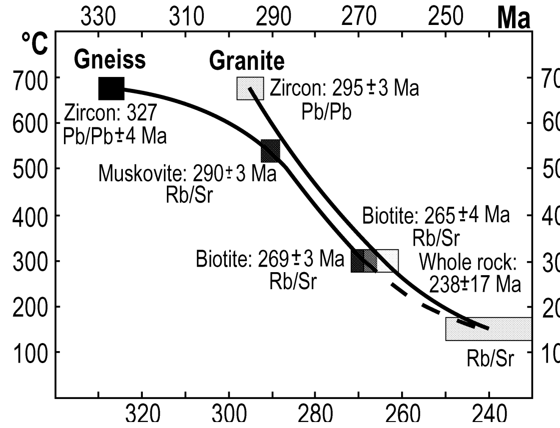

Fig. 6 Temperature/time-path for granites and gneisses of the gneiss-plate of Kartali

tinction. Rock units exhumed by erosion cool very slowly. They ascend by the same amount as the surface is eroded. Their cooling rates are below 10 K/Ma (Spear 1993). Tectonically exhumed complexes have a much higher cooling rate, because they have moved along faults into the neighbourhood of colder crust. They reach cooling rates of 25–75 K/Ma (Spear 1993). Plutons intruding cold country rocks reach cooling rates of up to 100 K/Ma (Spear 1993).

The temperature-time path of the gneiss-plate of Kartali was drawn for granites and gneisses respectively (Fig. 6). It shows not only the cooling of both rocks, but also their relation to each other. The protolith of the gneisses intruded in the middle crust 327±4 Ma ago and cooled very slowly with rates of 4–6 K/Ma during the next 30 Ma. This implies that it was not exhumed, but stayed at a hot middle crustal level until the intrusion of the Dzhabyk granite. The deformation of the gneisses at 290±3 Ma occurred at the same time as the intrusion of the Dzhabyk pluton. The cooling rate increased significantly to 8–14 K/Ma. The exhumation of the gneisses started. These facts give reason for the assumption that the deformation of the protolith of Kartali was caused by the intrusion of the pluton. Granites and gneisses ascended and cooled together. The gneisses reached a special cooling temperature always slightly earlier than the granites, because they form the marginal parts of the granite-gneiss complex. However, its lead decreased the more the temperature of the pluton equilibrated to its country rock.

Which mechanism of exhumation can be deduced from the temperature-time path? Erosion can be excluded, because the cooling rate is too high. Extremely strong erosion has never occurred in the Urals. Furthermore, the field data does not correspond with an exhumation by erosion, because erosion cannot uncover middle crust locally, while a few kilometres away almost non-metamorphic upper crust is exposed. Complexes that were exhumed along active faults have much higher cooling rates. The ascent of plutonic rocks in post-collisional settings is usually realized by diapirs or dykes. A diapir burns through the overlying rocks because of its low density and ascends with velocities of m/a, while magmas ascending in dykes are much faster and reach velocities of mm/s (Paterson et al. 1995). The low cooling rate, the exhumation of the gneisses during the intrusion of the voluminous Dzhabyk granite and the dragging of already crystallized rocks of the plutonic roof allow the assumption that the Dzhabyk granite-gneiss complex was a diapir, which is supported by field data such as the pluton concordant circular foliation of its margin and the domed host rock. The physical conditions for diapirism in the East Uralian Zone were outstanding, because it is composed of basic rocks that had a high density contrast to the granitic magma. The diapir stopped latest when it reached the sedimentary cover of the basic rocks, which is evident in the microstructures by the wane of deformation in 6 km depth. The final exhumation is not documented both in the microstructures and the investigated isotope systems.

We can conclude that the gneisses are deformed marginal parts of post-collisional granites and thus one of the youngest rocks of the Eastern Urals and not the oldest.

This interpretation is supported by Sr-Nd isotope data from the whole East Uralian Zone. However, not only the gneiss-protolith is too young to be deduced from the old continental crust. Even the magma source is too young to be part of the East European Craton, which is older than 1.65 Ga.

The τ_{DM} model ages of 700–1,200 Ma demand significant amounts of younger material for the generation of the gneiss protoliths.

This result requires a totally new geodynamic concept for the Urals. Since no evidence for an old microcontinent can be found in the East Uralian Zone, the collisional partner for the Uralian orogenesis is missing. Thus, it must be discussed as to what extent other rock units have participated in the Uralian crustal thickening.

Pre-Uralian age information

The Sr-Nd isotope data provides evidence that an island arc was the magma source of the granite-gneiss complexes. This implies that the island arc crust must have been extremely thickened during the Uralian orogenesis. How could that happen?

Ayala et al. (2000) report that short wavelength magnetic anomalies, which are characteristic for the Magnitogorsk Zone island are rocks, also can be found at the East European Craton. Schists from the Maksyutov complex coincide with this data. They indicate an island arc origin (Schulte & Blümel 1999) and yield zircon ages from 800–1,300 Ma (Hetzel 1999). This data gives evidence for the existence of pre-Uralian island arc complexes at the eastern margin of the East European Craton. Furthermore, a Devonian island arc is exposed in the Magnitogorsk Zone. The crustal thickening can be explained by two mechanisms: the stacking of the Magnitogork island arc or the westward thrusting of the Mag-

Fig. 7 Isotope data indicating Pre-Uralian events in the southern Urals

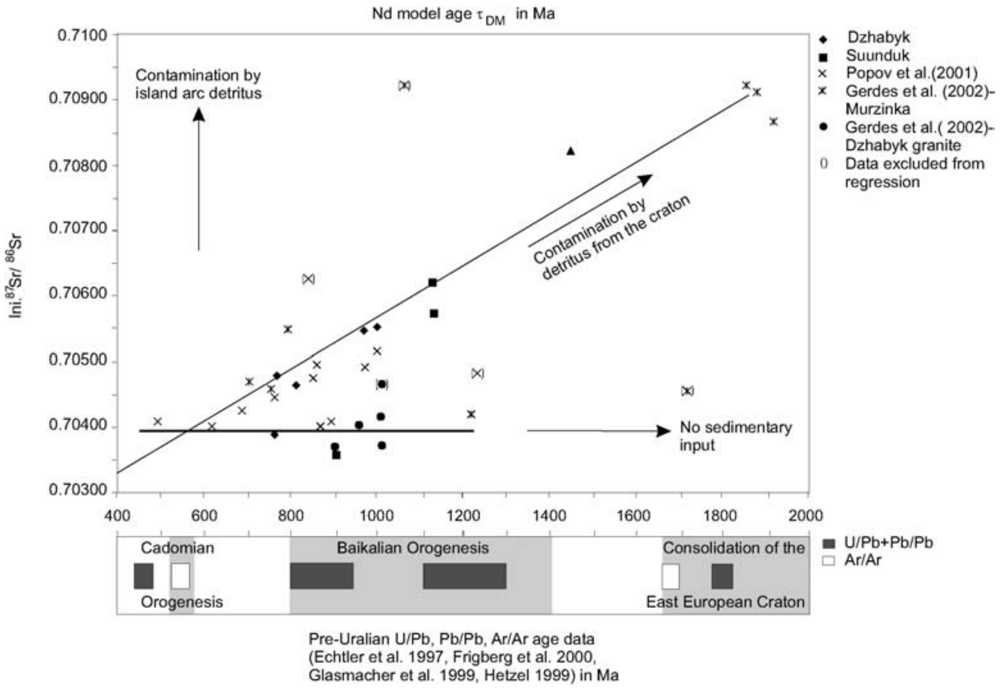

nitogorsk island arc over the pre-Cambrian island arc units.

A geodynamic model describing the Uralian orogenesis has to support one of these two mechanisms. Therefore, it is desired to characterize the magma source using the data from Gerdes et al. (2002) and Popov et al. (2001) in addition to our own data.

It has to be taken into account that an island arc is a heterogeneous magma source. It is composed of lower crustal tonalite-trondhjemite suites containing exclusively magmatic rocks and of upper island arc crust that consists of volcanic or volcanoclastic rocks and sediments. These sediments may have been eroded from the island arc itself or from the continental margin of the East European Craton.

The source of the granite-gneiss complexes consists of sedimentary and magmatic rocks (Gerdes et al. 2002) and was separated from the depleted mantle at 700–1,200 Ma. τ_{DM} model ages). It was affected by a middle Ordovician magmatic event (zircon ages).

Nd- model ages are minimum values for the separation of crust from the depleted mantle and increase when juvenile material is mixed with older crust. At the continental margin of the East European Craton it has to be taken into account that detritus was eroded from this site. It should have an age of >1.65 Ga because the consolidation of the craton was finished at this time (Giese et al. 1999).

To estimate the influence of the detritus from the East European Craton on the model ages of the granite-gneiss complexes we plotted the initial $^{87}Sr/^{86}Sr$-ratios of the samples against their τ_{DM} (Fig. 7). Rb and Sr fractionate by chemical weathering. Therefore, a higher percentage of sediments cause higher initial $^{87}Sr/^{86}Sr$-ratios. The Sm/Nd-ratio is resistant against weathering because of the nearly identical geochemical behaviour of both these elements. If island arc sediments are melted, only the initial $^{87}Sr/^{86}Sr$-ratios should increase. If sediments from East European Craton are melted the initial $^{87}Sr/^{86}Sr$-ratios and the τ_{DM} ages must increase. Since lower crustal island arc magmatic rocks do not contain significant amounts of sediments, low initial $^{87}Sr/^{86}Sr$-ratios must be expected and the τ_{DM} ages should date the real age of the separation of the sample from the depleted mantle.

As shown in Fig. 7 the data points follow two linear trends. Trend 1 shows a slightly positive correlation of the initial Sr-ratios and τ_{DM} ages. The initial $^{87}Sr/^{86}Sr$ ratios of all the samples of this group are nearly constant and low (0.704), which indicates almost no sedimentary contamination. We assume that these samples were generated from lower island arc crust. Trend 2 shows a positive correlation of Sr-ratios and τ_{DM} ages that point to a contamination of the source by older sedimentary material. The regression line of the data of this group can be interpreted as a mixing line between two components. Component 1 consists of sediments eroded from the East European Craton. They have high initial Sr-ratios and τ_{DM}>1.65 Ga. Component 2 has initial Sr-ratios of 0.704 and a τ_{DM} of 500–600 Ma and can be interpreted as an island arc magmatic rock. We can assume that the samples of group 2 represent melted upper crust of the island arc with varying contents of sedimentary material.

The points of group 1 can also be drawn by a regression line that intersects the regression line of group 2. The point of intersection marks the youngest possible age of the pre-Uralian island arc activity and lies at approximately [560 Ma, 0.70393]. It coincides with the age of the Cadomian orogenesis in the Urals, which was dated by Glasmacher et al. (1999) in the Beloretsk terrane.

For a geological interpretation we compared the model ages to age data from those geological units that expose pre-Uralian island arc rocks: the Maksyutov complex west of the Main Uralian Fault and the Sisert complex in the East Uralian Zone of the Middle Urals.

The Maksyutov Complex exposes the continental margin of the East European Craton that is covered by sediments with an island arc signature (Schulte & Blümel 1999). The protolith age of these island arc pelitic rocks was dated by several authors with the Rb/Sr and U/Pb method (Dobretsov 1974, Sobolev et al. 1986 and others in Hetzel 1999). They show a wide age spectrum of 800–1,300 Ma that coincides with the Baikalian orogeny. They were overprinted thermally 550–540 Ma ago (Matte 1993, Krasnobajev 1995 in Hetzel 1999) during the Cadomian orogeny. Furthermore, Ordovician microfossils were found in marble lenses (Ivanov et al. 1990 in Hetzel 1999). This sedimentary input was correlated with the rifting of the Ural Ocean (Hetzel 1999).

Metamorphic volcanic and sedimentary rocks, which are interpreted as island arc complexes, are exposed in the Sisert Complex. Their geochemical data are equal to that of the gneiss-plate of Kartali in some points. They were intruded by magmatic rocks at approximately 450 Ma. The τ_{DM} ages lie in the range of 564–1,033 Ma (Echtler et al. 1997). These island arc rocks were incorporated in the Uralian collision and experienced pressures of 6–10 kbar (Echtler et al. 1997).

We assume that the Maksyutov and Sisert Complexes expose the same crust that forms the magma source of the granite-gneiss complexes. A direct comparison of this age data is only possible with data from group 1, because they do not contain sedimentary components. The τ_{DM} ages fit the geochronological data described above. Both the τ_{DM} and the protolith ages of the Maksyutov Complex fall into the interval of 800–1,300 Ma and may be interpreted as results of the Baikalian formation of crust. Between 800 and 600 Ma there is a hiatus of both data sets. New signs of thermal activity can be found in both data sets at approximately 560 Ma during the Cadomian orogeny.

The thrusting of pre-Cambrian subduction-accretion complexes by the Magnitogorsk island arc during the Uralian orogeny as a mechanism of crustal thickening is therefore favoured. This interpretation contradicts the work of Gerdes et al. (2002), who favour a Devonian magma source, but it is supported by the occurrence of middle Ordovician magmatic zircons in the gneisses. These zircons verify that pre-Uralian magmatic rocks are part of the magma source and these pre-Uralian magmatic rocks must have crystallised in the pre-Uralian crust.

Conclusions

The gneisses of Kartali are possibly derived from the oldest parts of the Dzhabyk pluton. They crystallized in the Upper Carboniferous in 327±4 Ma in the middle crust and stayed there for 30 Ma almost without cooling. They have been deformed at 290±3 Ma ago at the same time as the Dzhabyk granite intruded and ascended diapirically (Fig. 8). This fact and the pluton concordant orientation of the gneissic foliation verify that the ascension of the pluton was the reason for the deformation of its roof. The Granites and gneisses cooled together, thus the gneisses of Kartali represent the strained margin of the Dzhabyk granite and not a part of an old microcontinent.

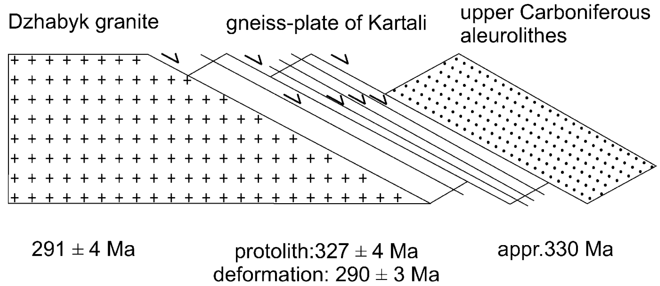

Fig. 8 The ages of rock units at the eastern margin of the Dzhabyk pluton. No indications for the existence of pre-Cambrian rocks have been found

Isotope data from Echtler et al. (1997), Gerdes et al. (2002) and Popov et al. (2001) are consistent with our data. They indicate that probably no old continental crust exists in the whole East Uralian Zone.

This means that the Uralian orogeny can no longer be interpreted as a continent-island arc-microcontinent collision, since the collisional partner is missing. Instead, the geochemical data presented within this paper indicates that the stacking and thrusting of Baikalian, Cadomian and Uralian island arc complexes played an important role during the Uralian orogeny. This should be considered in new models describing the geodynamic evolution of the Urals.

Acknowledgements We thank H. Baier and A. Braun for their laboratory assistance and support on the mass spectrometer and M. Bröcker supervising the laboratory work and data processing. We are grateful to Prof. Montero and Dr. Paquette for very careful review that helped to improve this paper considerably. The project was founded by the Deutsche Forschungsgemeinschaft, project KR1566/2-2 and the Saxon Ministry for Science.

References

Ayala C, Kimbell GS, Brown D, Ayarza P, and Menshikov YP (2000) "Magnetic evidence for the geometry and evolution of the eastern margin of the East European Craton in the Southern Urals". Tectonophysics 320:31–44

Benisek A, Finger F (1993) Factors controlling the development of prism faces in granite zircons: a microprobe study. Contrib Mineral Petrol 114:441–451

Berzin RG, Suleymanov AK, Puchkov VN, Shushukin YK, Ermolaeva GM, and Ostanina NV (2001) "Deep structure and geodynamics of the South Urals (project URALSEIS)". Ministry of Natural Resources of the Russian Federation, FGU GNPP, Spezgeofizika, Tver, pp 1–286 (in Russian)

DePaolo DJ, and Wasserburg GJ (1976) Nd isotopic variations and petrogenetic models. Geophys. Res. Lett. 3:249–252

Dobretsov NL (1994) Glaucophane schists and eclogite glaucophane-schist complexes in the USSR. Nauka Press, Novosibirsk, pp 1–429 (in Russian)

Dodson MH (1973) Closure temperature in cooling geochronological and petrological systems. Contrib Mineral Petrol 40:259–274

Döring J, and Götze H-J (1999) The isostatic state of the southern Urals crustal root. Geol Rundsch. 87/4:500–510

Echtler HP, Ivanov KS, Ronkin YL, Karsten LA, Hetzel R, and Noskov AG (1997) The tectono-metamorphic evolution of gneiss complexes in the Middle Urals, Russia: a reappraisal. Tectonophysics 276:229–251

Fershtater GB, Montero P, Borodina NS, Pushkarev EV, Smirnov VN, Bea F (1997) Uralian magmatism: an overview. Tectonophysics 276:87–102

Frigberg M, Larionov A, Petrov GA, and Gee DG (2000) Paleozoic amphibolite-granulite facies magmatic complex in the hinterland of the Uralide Orogen. Int J Earth Sci 89:21–39

Gerdes A, Montero P, Bea F, Fershtater G, Borodina NS, Osipova T, and Shardakova G (2002) Peraluminous granites frequently with mantle-like isotope compositions: the continental-type Murzinka and Dzhabyk batholiths of the eastern Urals. Geol Rundsch 91:3–19

Giese U, Glasmacher U, Kozlov VI, Matenaar I, Puchkov VN, Stroink L, and Walter R (1999) Structural framework of the Bashkirian anticlinorium, SW Urals. Geol Rundsch 87/4:526–544

Glasmacher UA, Reynolds P, Alekseyev AA, Puchkov VN, Stroink L, and Walter R (1999) ^{40}Ar/ ^{39}Ar Thermochronology west of the Main Uralian Fault, southern Urals, Russia. Geol Rundsch 87/4:515–525

Hetzel R (1999) Geology and geodynamic evolution of eclogite and associated garnet-mica shist in the high-pressure metamorphic Maksyutov complex, Ural, Russia. Geol Rundsch 87/4:577–588

Ivanov KS, Puchkov VN, Babenko VA (1990) Occurrences of conodonts and graptolites in the metamorphic sequences of the southern Urals. Doklady Akademii Nauk 310:676–679 (in Russian)

Jäger E (1973) Die alpine Orogenese im Lichte der radiometrischen Altersbestimmung. Ecolgae Geol Helvet 66:11–21Glasmacher UA.

Kisters AFM, Meyer FM, Seravkin IB, Znamensky SE, Kosarew AM, and Ertl RGW (1999) The geological setting of lode-gold deposits in the central southern Urals: a review. Geol Rundsch 87/4:603–616

Kober B (1986) Whole grain evaporation ^{207}Pb/^{206}Pb-age investigations on single zircons using a double-filament thermal ion source. Contrib Mineral Petrol 93:482–490

Kober B (1987) Single-zircon evaporation combined with Pb+ emitter bedding for 207Pb/206Pb-age-investigations using thermal ion mass spectrometry and implications for zirconology. Contrib Mineral Petrol 96:63–71

Kramm U, Chernyshev IV, Grauert B, Kononova VA, and Brücker W (1993) Zircon typology and U-Pb systematics: a case study of zircon from Nepheline Syenite of the Il'meny Mountains, Urals. Petrology 1:474–485

Krasnobajev AA Davudow BA, Lennykh VI, Tscherednitschenko NB, Koslow WJ (1995) The age of zircons and rutiles from the Maksyutov Complex (preliminary data). Ezhegodnik 1995, Yekaterinburg, pp 13–16 (in Russian)

Ludwig KR (1999) Isoplot/Ex-vers.2.06: A geochronological toolkit for MS-Excel. Berkeley Geochronology Center Special, Publication No. 1a, pp 1–46

Matte P, Maluski H, Caby R, Nicolas A, Kepeshinskas P, Sobolev S (1993) Geodynamic model and 39Ar/40 Ar dating for the generation and emplacement of the high pressure (HP) metamorphic rocks in SW Urals. C R Acad Sci 317:1,667–1,674

Montero P, Bea F, Gerdes A, Fershtater G, Zin'kova E, Borodina N, Osipova T, and Smirnov V (2000) Single- Zircon evaporation ages and Rb-Sr dating of four major Variscan batholiths of the Urals — A perspective on the timing of deformation and granite generation. Tectonophysics 317:93–108

Paterson SR, Fowler TKJr., and Miller RB (1995): Pluton Emplacement in Arcs: A Crustal-Scale Recycling Process. USGS Circular 1,129:111–112

Popov WS, Bogatov WI, and Shurawlev DS (2001) Wosmoshnuije istotschniki gerzinskich granitnuich porod ushnowo Urala: Rb-Sr i Sm-Nd isotopnuije dannui. MGGA, IMGRE: 168–171

Poty E, and Roth B (1989) Nuclear Methods of Dating, Solid Earth Science Library. Kluwer Academic Publishers

Pupin JP (1980) Zircon and Granite Petrology. Contrib Mineral Petrol 73:207–220

Schulte BA, and Blümel P (1999) Metamorphic evolution of eclogite and associated garnet-mica schist in high-pressure metamorphic Maksyutov complex, Ural, Russia. Geol Rundsch 87:561–576

Sengör AMC, Natal'in BA, and Burtman VS (1993) Evolution of the Altaid tectonic collage and Palaeozoic crustal growth in Eurasia. Nature 364:299–307

Shenderowitsch DM (1965) Comments on the geological map of the Suunduk complex, departement of geology of Orenburg. (in Russian)

Sobolev NV, Dobretsov NL, Bakirov AB, Shatsky VS (1986) Eclogites from various types of metamorphic complexes in the USSR and the problem of their origin. In: Evans BW, Brown EH (eds) Blueschists and eclogites. GSA Mem 164:349–363

Spear FS (1993) Metamorphic Phase Equilibria and Pressure-Temperature-Time Paths. Mineralogical Society of America, Washington DC, pp 729–735

Stacey JS, and Kramers JD (1975) Approximation of terrestrial lead isotope evolution by a two stage model. Earth Planet Sci Lett 26:207–221

White WM (1997) Geochemistry, Ithaca, NY, Cornell University, internet publication (world wide web).